NEW CONSIDERATIONS FOR TRAVELING WAVE PARTICLE HANDLING

Felix M.Moesner [1, 2], Toshiro Higuchi [2, 3] and Yoshikazu Tanii [2, 4]

[1] *Swiss Federal Institute of Technology Zurich • Institute for Robotics*
ETH Center / CLA, 8092 Zurich, Switzerland • Fax: +41 1 632 1078 • Email: moesner@ifr.mavt.ethz.ch

[2] *Kanagawa Academy of Science and Technology • Higuchi 'Ultimate Mechatronics' Project*
KSP Bldg., East 405, 3-2-1 Sakado, Takatsu-ku, Kawasaki 213, Japan • Fax: +81 44 819 2095

[3] *University of Tokyo • Department of Precision Machinery Engineering*
Hongo 7-3-1, Bunkyo, Tokyo 113, Japan • Fax: +81 3 5800 6968

[4] *Pure Material Laboratory Ldt.*
5-30-1 Kumegawa-cho, Higashimurayama City, Tokyo 189, Japan • Fax: +81 423 94 4500

***Abstract* – Different small-scale devices for particle micro-handling using an AC electric field boundary wave were proposed by [Moesner et al., 1]. These devices, with various novel transportation and manipulation features, that instantly generate particle driving forces through electric field creation, have been designed and produced. In a further endeavor, the mechanisms of particle conveyance are here subsequently validated in experiments.**

Particles on a thin protecting and insulating film interface above a series of encased and insulated parallel field electrodes become either tribo-electrically or induction charged through the application of balanced three- or six-phase voltages. The created non-uniform traveling field-wave conveys the charged particles perpendicular to the electrodes by repulsive forces in a hopping mode from electrode to electrode.

In a temperature and humidity controlled environment, experiments surveying particle conveyance dynamics on these electric devices have been carried out with help of a high speed camera. The applied experiment voltages included triangular, ramp and two customized profiles. Various particle materials with diameters up to 400 µm have been examined; metal, glass, and plastic spheres showed the best performances. The transient charge distribution on particles and on the activated electric device, which is responsible for the particle conveyance, has been inspected by a modified scanning electron microscope (SEM). Further, theoretical considerations underline the experimental findings.

I. INTRODUCTION

In modern industry, there are several implemented techniques employed for particle handling. Each technique is suited to a particular goal in the process and also may take advantage of a specific particle property. These handling methods include classical air- and fluidborne transportation by regulated carrier gas or liquid flow. Particles are conveyed in bulk in long flexible tubes and pipes, as described by [2]. This purpose-oriented guidance of a mass of particles to a fixed target container, render micro-manipulation of single objects nearly impossible. Similarly, transportation by surface vibrations carries a bulk of particles to a fixed spot. Apparatus incorporating this technique form the group of parts feeder which was conceived purely for mass transportation and not for the controlled micro-manipulation of objects.

In some cases, an explicit particle-property is set as conveyance trigger. [3] and [4] demonstrate the usage of magnetic fields to manipulate fine magnetic particles. High gradient magnetic separation enables even the effective handling of very weakly magnetic particles of micron size as published in [5]. The advantage lies in the property-oriented separation of particles into two different groups of magnetic and non-magnetic objects. However, this technique prevents the handling of purely non-magnetic particles.

In contrary to above methods, it is conceivable to use tiny grippers or shovels for single particle manipulation. The goal of these systems is to handle and assemble micro structures. [6] reports a solution to the grasping and holding of small particles or cells by microgrippers. A nanorobotic system which was assigned the task of automated handling of micro-parts with nanometer resolution is described in [7]. This goal-oriented method allows manipulation of single particles despite their different properties.

Listed methods are related by the common application of particle handling. However, they are all together restricted to a particular range of handling abilities, such as bulk transportation, single handling or property-oriented manipulation. With the appropriate use of *electrostatic* forces however, it is possible to create very compact devices for particle handling, possessing advantages over the above mentioned methods and therefore providing good alternatives.

The method of using electrostatic forces for particle handling has already been outlined in various papers and proven in applications. DC electrostatic forces were engaged in surface cleaning and particle dispenser processes as presented in [8]. Transportation of fine particles by a three-phase traveling electric field was originally proposed in [9] in the early seventies. The discovery has been reported as an *electric curtain*, where aerosol particles are continuously levitated against gravity. Frequency and phase-lag effects on fine

IEEE Industry Application Society Conference Record, 31st Annual Meeting
San Diego, October, 1996, pp. 1986 - 1993.

particle transportation for the electric curtain mode have been theoretically studied by [10], where systems with wide electrode gaps have been proposed. Linear motion of microscopic objects was done by [11], and manipulation of cells in [11] and [12].

This paper focuses on devices for particle transportation and manipulation in the interface between the micro- and macro-world by making use of AC electric fields as the contactless particle conveyor. By this technique, a diverse range of particle substances showed an effective frequency dependent transportation performance. The devices are connected to and activated by a multi-phase, programmable, high voltage supply with a profile amplitude range of up to 2 kV_{ptp}. The energizer electrodes integrated into the devices are situated at equal distance to each other and possess different designs, such as parallel or dot-shaped conductors.

Since no moving machine parts are involved, the forces of the electric field can reduce overall energy consumption. It is expected that the described approaches will lead to new applications in various fields, such as a parts feeder and manipulator for micro electro mechanical systems (MEMS).

II. Principle of Conveyance

To explain the traveling wave principle, only slim and long parallel electrodes with a constant gap, which form the skeleton of the *electric panel*, shall be considered in the following interpretation.

Balanced, multi-phase high voltages from a programmable source are supplied to a series of encased, parallel electrodes which are covered and protected against electrical breakdown by a thin insulating film. Upon the activation of the electrodes, a traveling electric field is created around the electrodes which is transiently changing with the applied voltage phase.

Particles on the thin insulating film interface above the encased and insulated parallel field electrodes become, depending upon the material, either triboelectrically or induction charged through the application of voltages to the electrodes. Dynamic forces from the created non-uniform traveling field-wave overcome the adhesion and gravitational forces of the charged particles and convey them in a direction in the plane perpendicular to the electrodes in a hopping mode from electrode to electrode.

A multi-channel, programmable, high voltage supply is attached to the electric device, where every sixth electrode belongs to the same phase state: *a*, *b*, *c*, *d*, *e*, or *f*. Figure 1.1 shows the principle of the electrode connection to each phase.

The supply sequence from the voltage source to the electrodes is given in Table I. Considering balanced square profile voltages, for a better understanding, the sequence is written with [+], [0], and [-] for a three- and a six-phase supply representing the 3 voltage states. The six-phase case requires all of the 6 attachments, whereas in the three-phase case, *a* and *d*, *b* and *e*, *c* and *f* are connected to the same phase. Particle transportation occurs with the variation of the sequence, i.e. the particle synchronously moves with one phase. As a consequence, within one six-phase period, the particle is conveyed along a distance double that of one three-phase period. Different types of balanced high voltage profiles are utilized, such as sine, square, triangular, etc. waves, each having a different effect on the particle conveyance dynamics.

Particles involved in the experiments were in the 5 µm to 400 µm diameter range. Various metals, glass, and plastic spherical particles gave the best results in a series of conveyance tests. A selection of 70 different types of substances have been examined, and about half of the tested particle materials showed an acceptable frequency dependent transportation behavior. Raising the frequency above the 100 to 200 Hz range, caused the particle movement to cease with our employed devices. It has been observed that spherical particles smaller in diameter than the pitch-length were

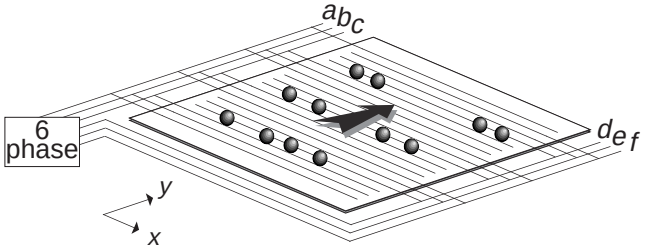

Fig. 1. Electrode connection to each of the six phases *a, b, c, d, e,* and *f.*

TABLE I
6 Electrode Attachments *a, b, c, d, e,* and *f* and their Supply from a Multi-Phase Voltage Source

Sequence ↓

a	*b*	*c*	*d*	*e*	*f*
+	-	0	+	-	0
+	0	-	+	0	-
0	+	-	0	+	-
-	+	0	-	+	0
-	0	+	-	0	+
0	-	+	0	-	+

Supply sequence of three-phase square profile voltages

a	*b*	*c*	*d*	*e*	*f*
+	+	0	-	-	0
0	+	+	0	-	-
-	0	+	+	0	-
-	-	0	+	+	0
0	-	-	0	+	+
+	0	-	-	0	+

Supply sequence of six-phase square profile voltages

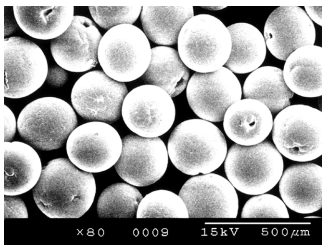

Fig. 2. A SEM micrograph of representative spherical *Fe*-particles.

suitable for conveyance in most of the experiments. For the following experiments, we focused on the usage of spherical, metal and glass particles. Representative samples are shown in Fig. 2.

III. Electric Panel Devices: Fabrication

As shown in the cross-sectional view of Fig. 3, the *electric panel* device is composed of parallel electrodes encased in epoxy resin, an insulating thin cover-film, a supporting panel, and electrode-attachments to the phases of the power supply. It is important to guarantee sufficient insulation between the electrodes which can resist an electric field strength of 57 kV/cm or more.

The parallel electrodes of the *electric panel* have an average center-to-center pitch length of 400 µm, a diameter of 50 µm and are situated parallel to the surface at a distance of 25 µm to 75 µm. The *electric panel* represents the most compliant device. Due to the simple electrode design, more flexibility can be added to the device by increasing the number of connectable voltage phases. Six is directly dividable by two and three, so it is conceivable to use one and the same device with a six-phase attachment in a two- or three-phase mode.

Fig. 4 shows the perspective view of an *electric panel* for bi-directional particle transportation. The particles are conveyed rectangular to the electrodes in one direction across the entire surface and by reversing the voltage supply sequence, the particles are transported in the other direction.

An approach to achieving two-dimensional particle handling is shown in Fig. 5. A second electrode layer perpendicular to the first can be added with a sufficient insulation gap between them. Alternatively, a mesh interweaving the two layers can be employed as shown in Fig. 6 and utilized in the *electric panel* described and employed herein. In order to endure high voltage differences at the nodal points which can be as high as 666 kV/cm, individual mesh-electrodes must be covered with a sufficient insulation such as polyamide-imide. This insulator assures a dielectric strength of up to 2756 kV/cm under ambient conditions. Particles can be conveyed two-dimensionally over the entire surface; this includes tetra-directional motion when the two electrode sets are activated separately. Octal-directional manipulation is reached by the combined energizing of the two sets.

A view of the real *electric panel* is kept as a picture in Fig. 6. The field electrodes possess a voltage supply at one end and remain insulated at the other. By this structure, the electrodes function as capacitors with a capacitance of approximately 260 nF in the employed frequency range. The total particle manipulation surface has dimensions of 100 mm in width and 75 mm in height. A section of the surface is magnified and represented as a SEM image. It illustrates the mesh structure of the field electrodes. The entire panel is covered by a thin film and hermetically seal by epoxy resin in order to increase safety during operation.

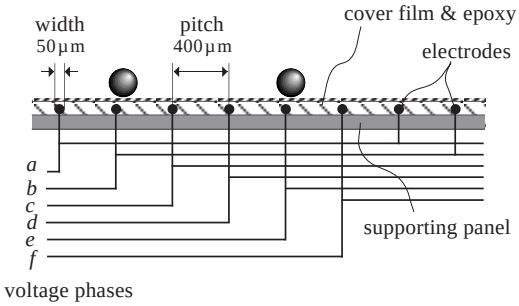

Fig. 3. Cross-section of the *electric panel* revealing its structural composition. Every sixth electrode is attached to the same phase.

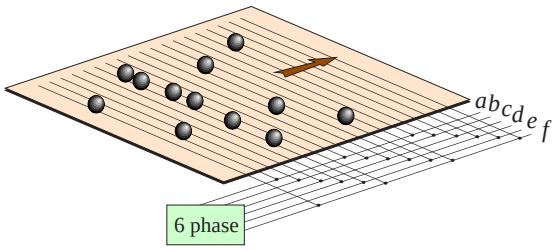

Fig. 4. *Electric panel* for bi-directional particle transportation perpendicular to the electrodes.

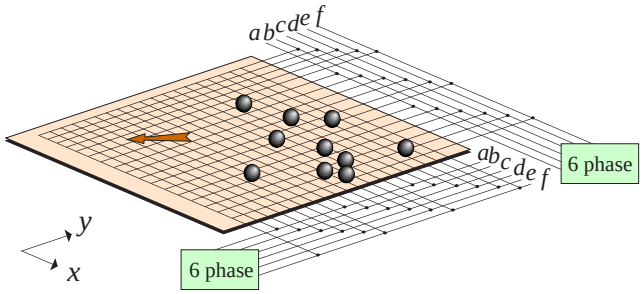

Fig. 5. *Electric panel* for tetra- and octal-directional particle handling. Highly insulated electrodes are woven to a mesh.

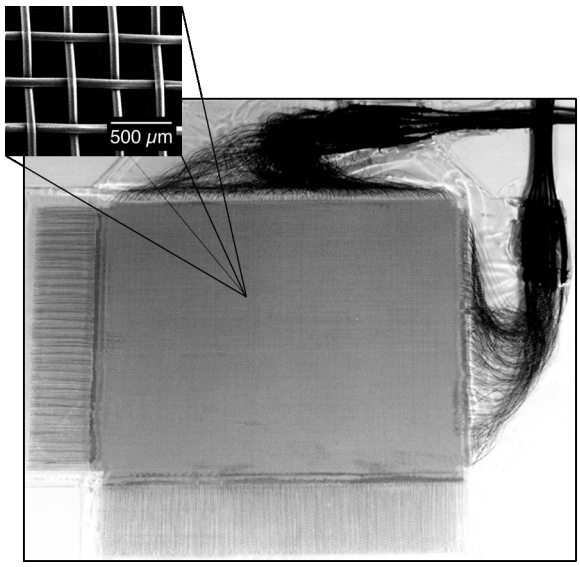

Fig. 6. *Electric panel* with magnified mesh-structure of the electrodes.

IV. Potential Distribution of Electric Fields

In experiments with small particles, panels are employed in various actuation modes such as three- and six-phase. Furthermore, the individual single phase voltage is of a particular wave profile such as sine, pulse, triangular or other. It is now of interest to obtain the potential distribution of the electric fields over and in an *electric panel*. The focus of the following calculation is the pulsed wave profile.

A. Calculation

Finding the potential distribution in the region between two conductors, given the charge distribution on the surfaces of the conductors or the potentials of the conductors or a combination of the two, is a problem for which Laplace's equation (1) can be used. In our case, we shall consider the solution of the two-dimensional Laplace equation (2).

$$\nabla^2 V = 0 \tag{1}$$

$$\frac{\partial^2 V}{\partial x^2} + \frac{\partial^2 V}{\partial y^2} = 0 \tag{2}$$

Generally, an equation of this type is solved by the analytical technique, the *separation of variables*. However, it has been considered to employ a numerical solution in order to take advantage of a computer. The method, which is explicitly described in [13], derives the finite-difference approximation. The *finite-difference method* is the basis for this computer solution.

14 mesh-electrodes of the *electric panel* have been defined in a matrix and connected to their appropriate phase *a, b, c, d, e,* and *f*.. The matrix is traversed iteratively by means of the finite-difference approximation until the computed error is smaller than a defined constant.

B. Results

The computational calculations of the potential distribution are shown in Fig. 7 and 9 in graphical form. The applied phase-voltage values are listed in Table II.

TABLE II
PHASE VOLTAGES USED IN POTENTIAL DISTRIBUTION CALCULATIONS.

three-phase voltages	six-phase voltages
a = 0 V	*a* = -10 V
b = -10 V	*b* = 0 V
c = 10 V	*c* = 10 V
	d = 10 V
	e = 0 V
	f = -10 V

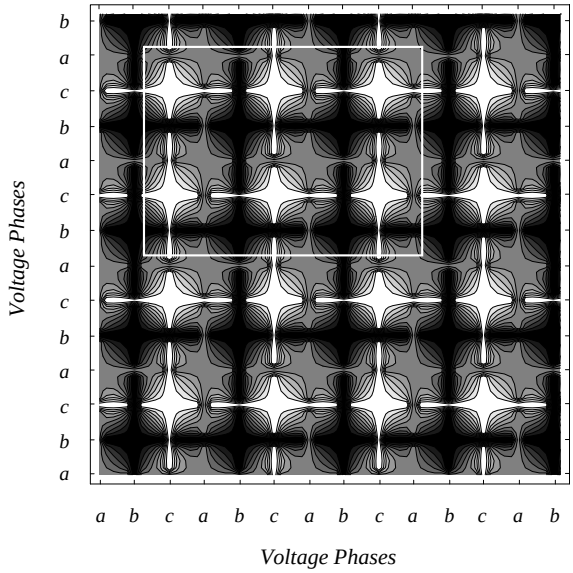

Fig. 7. Potential field calculation of an *electric panel* with three-phase voltage supply.

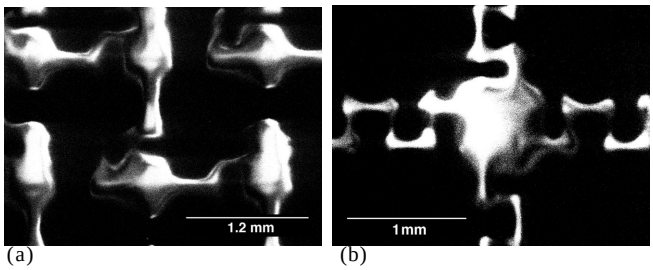

Fig. 8. SEM micrographs of an activated *electric panel*. The left segment is three-phase, the right is supplied by six-phase voltage.

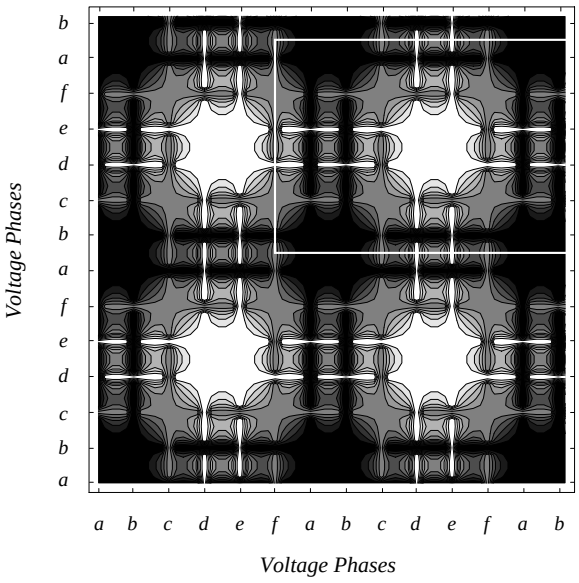

Fig. 9. Potential field calculation of an *electric panel* with six-phase voltage supply.

The result in Fig. 7 refers to the graphical computation of a three-phase case. The graph in Fig. 9 is obtained by a potential distribution calculation of a six-phase voltage supply to the electrodes. In both diagrams, the same three- or six-phase supply sequence has been chosen for the other activation dimension. As a result, a checker board pattern is obtained. The potential of each electrode has been kept in the range of ±10 V. The white and black areas represent the 10 V and -10 V level respectively. The number of equidistant layers is 9 between the minimum and maximum potential.

The two SEM micrographs of Fig. 8 depict the charge distribution on an activated *electric panel*. The SEM works as a charge distribution sensor and has therefore been modified to hold our experimental device. The white parts in the image represent the negative charge on the surface. Positive charge is not detected by the SEM and therefore appears black. Since charge and potential is considered to be analogous, the SEM images can be compared directly with the potential distribution calculation of Fig. 7 and 9. White frames have been shown to visualize a place where the SEM images fit into. It is not difficult to apprehend a good agreement with the overall pattern-structure.

A clear difference between the white areas of Fig. 7 and 9 is the size. The energizing pattern of three-phase voltages produces small, but more numerous activation areas as compared to the six-phase pattern where the activation areas are approximately 4 times larger, but also 4 times fewer in number on the same sized surface. This circumstance reflects the observation of different particle conveyance mannerisms for the three- and six-phase case independently of the wave profile. It has been noted that a larger activation area is responsible for transportation of larger particles than a smaller area. On the contrary, it appears that smaller activation areas allow more sophisticated handling of particles.

The potential distribution calculation in Fig. 9 corresponds very well with the checker board pattern of conveyed particles in Fig. 10. The white frame visualizes the location which the computed graphic of Fig. 9 matches. The photograph does not disclose particles which are positively or negatively charged. They are simply attracted to the black and white activated areas of Fig. 10. One activated node area is shown by a SEM image in Fig. 11; it is very clear to comprehend that the particles are attracted to and concentrated in an energized spot.

V. Observation of Particle Conveyance

The usage of a modified SEM opens many possibilities not only for the static observation of charge distribution on activated electric devices, but leads to the dynamic observation of traveling charge distribution and particle conveyance. For this purpose, a few particles have been positioned on the manipulation surface.

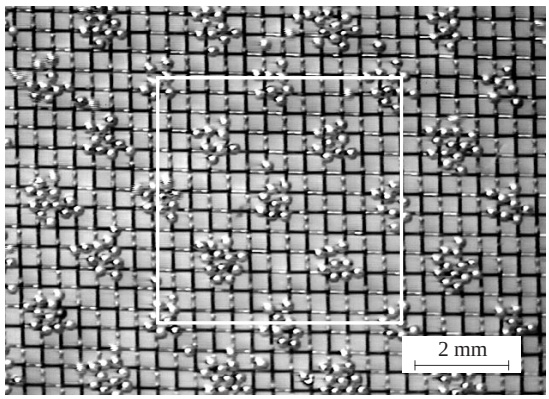

Fig. 10. Checker board pattern groups of conveyed particles on panel.

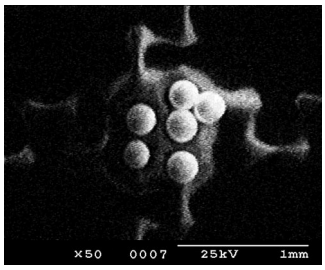

Fig. 11. SEM image of *Fe* particles attracted to an activated mesh area.

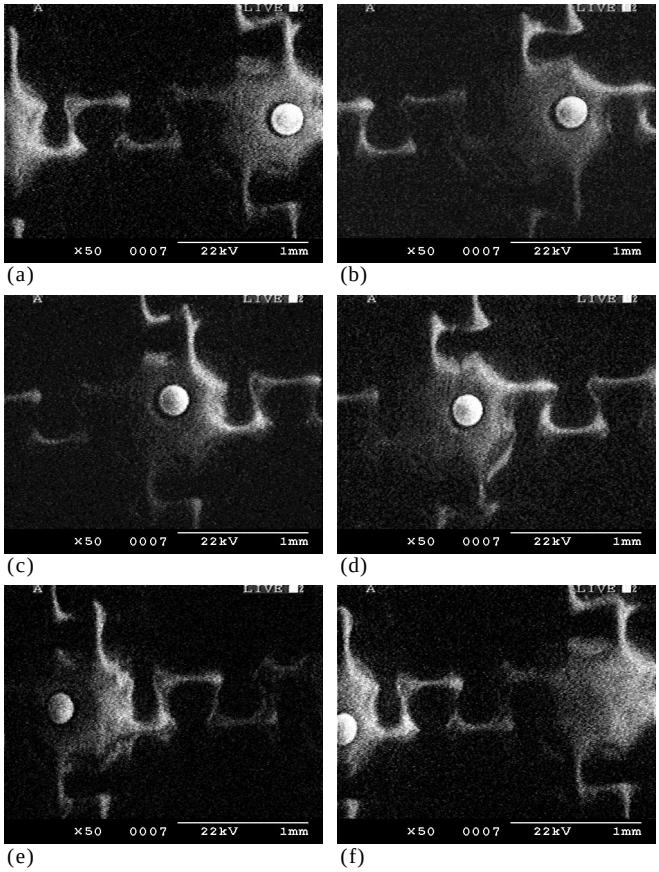

Fig. 12. Dynamic sequence of SEM images revealing tracked conveyance of a single particle from right (a) to left (f).

The motion was captured in the TV mode of the SEM. The sequence in Fig. 12 is the result of a single particle following the traveling field wave of a six-phase supply. It should be noted, that the particle uses the *tracked conveyance technique*, which is described in detail in [1]. Specifically, the track holds the particle on a line, which is visible as a static charge distribution in the recorded sequence of Fig. 12. The perpendicular electrodes actuate the particle. The sequence reveals how the particle moves step by step over a length of 6 electrode-pitches. The distance is about 2.0 mm. This sequence from (a) to (f) illustrates two facts: first, the particle is conveyed by the electric field of the AC activated electrodes and second, the particle is kept on a line by the DC energized electrodes.

VI. ELECTRIC DOTS DEVICE

A. Fabrication

The *electric dots* and *panel* device consist of a very similar structure and are functionally closely related. The main difference is the shape of the field electrodes. They are designed as long parallel electrodes in the panel, but as tiny dots in the other device. The effect of the traveling electric field is the same, but the positioning of the particles is more individual and precise with the dot matrix. Fig. 13 illustrates the structure of the dot matrix device. All electrodes are embedded in epoxy resin. Their terminal ends are cut perpendicularly and form, together with the body, a manipulation surface. The individual field electrodes are connected to their corresponding voltage phase. In practice, a sandwich structure of neatly cut *electric panel* layers delivers the desired dot electrodes in a matrix configuration. The SEM photo in Fig. 14 depicts the dot electrodes in the manipulation surface, which are visibly composed like a sandwich. Our realized matrix has a (6 x n)-dimension, i.e. it consists of 6 rows. The two central rows are responsible for particle actuation and the remaining four peripheral rows provide a potential track for the particles through their DC activation. The dots in the SEM picture of Fig. 14 are horizontally activated allowing the wave to travel either from left to right or vise versa.

B. Phase Lag

One effect which has been observed in experiments and theoretically described in [10] is the phase-lag between the advancing traveling electric field and the conveyed particle. It has been be noted that the particle still remains at a location while the traveling field wave is proceeding. A dynamic sequence of SEM images is shown in Fig. 15. It exposes the close-up actuation of a group of 100 µm glass particles in the direction of the inserted arrow on the manipulation surface of an *electric dots* device. A three-phase electrode activation has been chosen to pay attention to this effect in more detail.

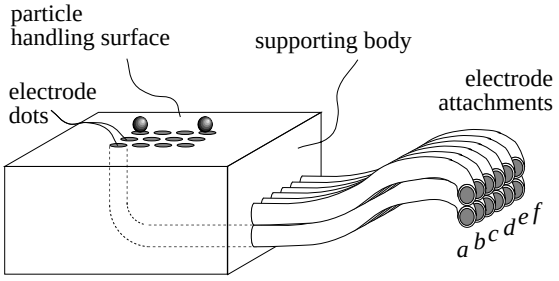

Fig. 13. Perspective of the *electric dots* device. The field electrodes are embedded in a epoxy resin body and connected to their phases.

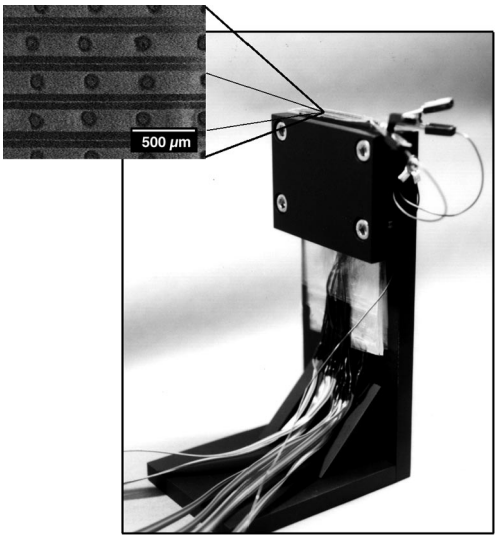

Fig. 14. Experimental setup of the *electric dots* device. The handling surface is at the top and magnified by a SEM image revealing its matrix dot electrodes in a sandwich structure.

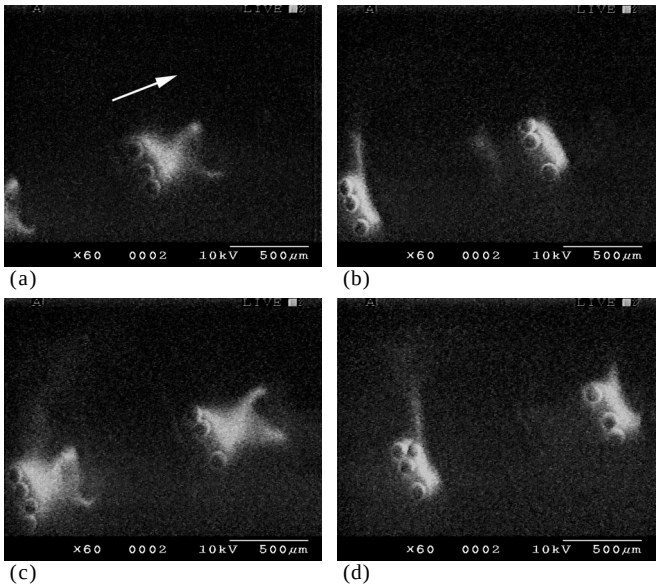

Fig. 15. Dynamic sequence of SEM images revealing the actual phase-lag between traveling field and conveyed particle. The glass particles show an actuation in direction of the arrow.

In (a), the particles remain on a particular spot while the field travels to the next location; then the particles follow (b) and stay again (c) while the field is proceeding. Finally, they follow on as shown in (d). This effect appears as particles try to find a balance between the transiently changing repulsive and attractive forces of the traveling field-wave.

VII. Hopping Height

The dynamic particle conveyance characteristic includes the hopping height as an assigned element when particles move stepwise from electrode to electrode. The following experiment has the aim to examine the hopping height while particles are conveyed towards an film layer verge. *Fe* particles with an average diameter of 250 µm were employed in this observation. As depicted in Fig. 16, a number of particles are barred by the edge of a film (a); whereas most of the particles were successful in surmounting the fringe in (b) – only a few were left behind. Three variables were taken into account: the thickness of the film layer, the applied voltage amplitude and the frequency. The rim of the film layer is positioned exactly between two electrodes. It is the location of expected maximal hopping height of an actuated particle. It is believed that the repulsive force is accountable for the major part in this hopping nature.

Several experiments were carried out at the ambient atmospherical condition of 20˚C and 30% RH. The *electric panel* with an electrode pitch of 400 µm has been activated by six-phase pulse voltage profiles as introduced in Table I. The averaged results are revealed in Fig. 17. The first graph (a) depicts the rate of successful particles overcoming the film fringe of 5 µm. At a low voltage of ±100 V, the frequency of approx. 13 Hz shows the highest rate, which is easily increased by raising the applied voltage. The phase voltage of ±250 V shows a rate of even more than 95 % above 5 Hz which indicates that many particles jump even higher than 5 µm. The hopping height diminishes in relation to a higher applied frequency. The rate of particles overcoming the 25 µm edge is represented in (b) – here, the frequency dependent hopping height can be easily seen. Increasing the applied voltage allows particles to hop over a fringe height of 50 µm (c) and even 100 µm (d). A height reduction by an increased frequency could hardly be conceived within the examined range.

VIII. Phase Voltage Profile

Under the condition of six-phase voltage supply, four different voltage wave profiles were produced by a digital signal processor (DSP) system and applied to the *electric panel*. These include triangle, ramp and two customized profiles as shown in Fig. 18, but with a voltage of ±500 V and frequency of 2 Hz. Each profile has a different effect on the particle actuation dynamics.

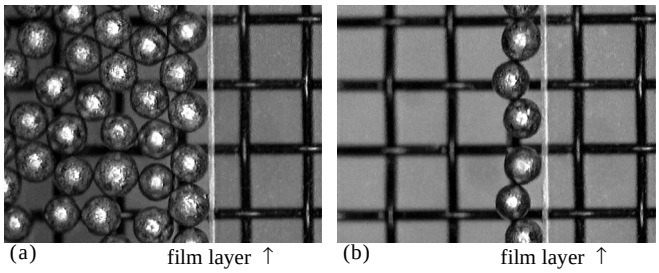

Fig. 16. Experiment used for observation of particle hopping height during conveyance. Film layer fringe in (a) stops most of the test particles, whereas in (b) only few are left.

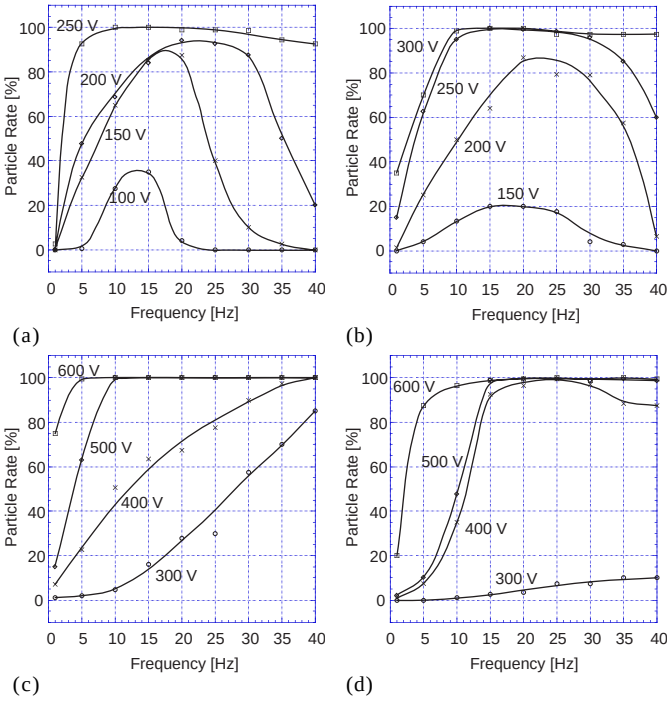

Fig. 17. Graph of successful particles versus frequency at various excitation voltages. Film layer heights: (a) at 5 µm , (b) at 25 µm, (c) at 50 µm and (d) at 100 µm.

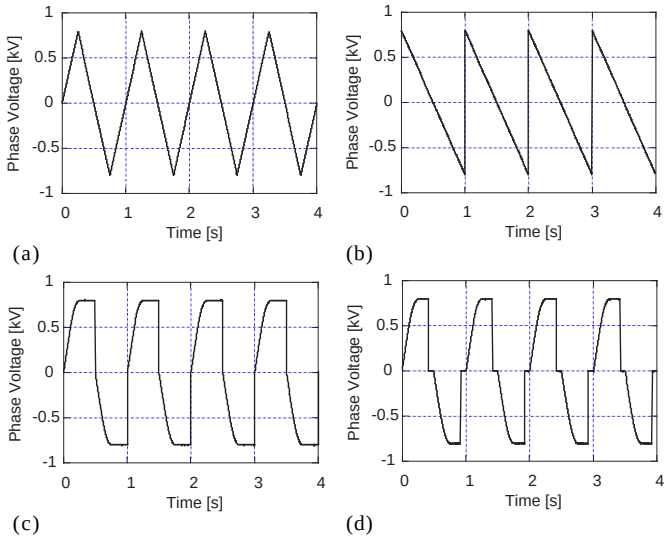

Fig. 18. Triangle (a), ramp (b) and two custom (c) & (d) wave profiles.

Fe-particles of 250 µm diameter were monitored by a high speed camera recording at a frequency of 4.5 kHz over a time span of 1.0 s and a distance of 5 mm. The ambient atmospherical condition was 20˚C and 30% RH.

The resulting conveyor characteristics in the *x*- and *y*-direction are shown in Fig. 19 for normal, untracked particle conveyance. Since the particles were not kept on an activated line, high conveyance fluctuation is clearly visible in the *x*-displacements. The particle proceeding stepwise from electrode to electrode is depicted in the *y*-displacement. The triangular profile excitation in (a) shows a similar behavior as the sine wave profile examined in [1]. The ramp profile in (b) presents a clear particle proceeding from electrode to electrode. The customized profiles are a mixture between sine and pulse profiles. They have been designed to unite the best qualities of both. The *x*-displacement in (c) reveals an oscillation which could be minimized in (d). This effect could be reached by inserting a zero level step into profile (c); the result is (d).

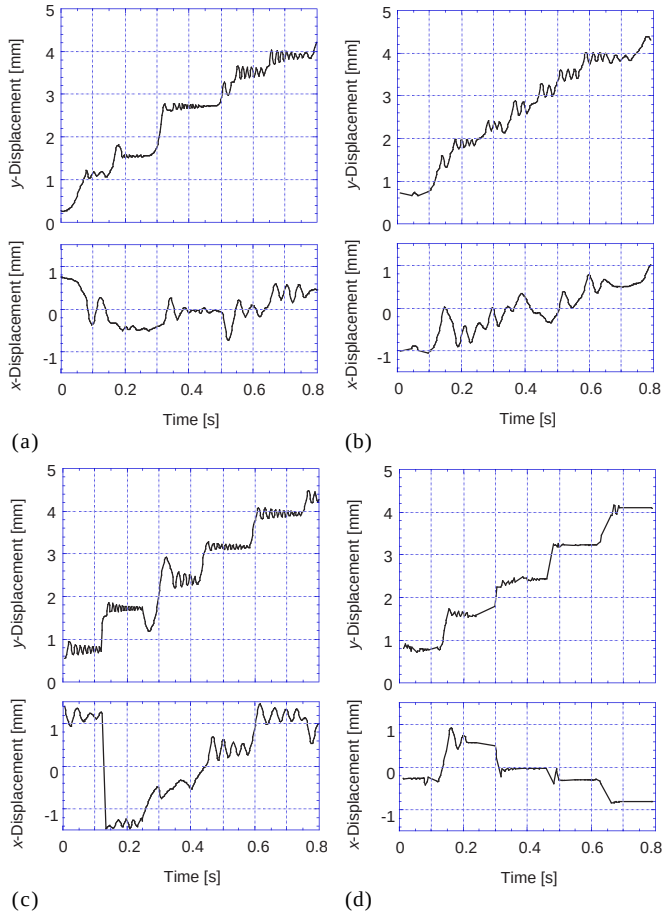

Fig. 19. Dynamic particle conveyance characteristics excitated by a triangle (a), ramp (b) and two custom (c) & (d) wave profiles.

IX. Conclusion

The potential distribution of electric fields in a three- and six-phase mode has been calculated and validated with charge distribution SEM images. Both results show very good agreement. The particle conveyance mechanism has been further explained by two SEM image sequences where the phase-lag between traveling wave and particle is commented. As part of the dynamic conveyance characteristic, the particle hopping height is observed and discussed. Finally, particle dynamics are captured by a high speed camera under excitation of triangular, ramp and two customized wave profiles.

Acknowledgment

We wish to acknowledge the appreciated and valuable collaboration of our colleagues S. Yashiro and A. Fujita for their engagement in some electric devices, S. Egawa and T. Niino for their expertise on voltage supply systems, J. Jin and S.J. Woo for prolific discussions, and W. Yang for his contributory involvement in this project.

References

[1] **Moesner**, F.M., and **Higuchi**, T., "Electrostatic Devices for Particle Micro-Handling," *IEEE Industry Applications Society*, 30th Annual Meeting, Orlando, vol. 2, 10 October, 1995, pp. 1302-1309.

[2] **Masuda**, H., **Komatsu**, T., and **Iinoya**, K., "The Static Electrification of Particles in Gas-Solids Pipe Flow," *AlChE Journal*, vol. 22, no. 3, May 1976, pp. 558-564.

[3] **Alward**, U., and **Imaino**, W., "Magnetic Forces on Monocomponent Toner," *IEEE Trans. Mag.*, vol. MAG-22, 1986, pp. 128-134.

[4] **Jones**, T.B., **Whittaker**, G.L., and **Sulenski**, T.J., "Mechanics of Magnetic Powders," *Powder Technol.*, vol. 49, 1987, pp. 149-164.

[5] **Oberteuffer**, J.A., "Magnetic Separation: A Review of Principles, Devices, and Applications," *IEEE Trans. Mag.*, vol. MAG-10, 1974, pp. 223-238.

[6] **Greitmann**, G., and **Buser**, R.A., "Tactile Microgripper for Automated Handling of Microparts," *Sensors & Actuators: A. Physical*, vol. SNA 053 / 1-4, 1996, pp. 409-414.

[7] **Codourey**, A., **Zesch**, W., **Büchi**, R, and **Siegwart**, R., "A Robot for Automated Handling in Micro-World," *IROS'95 IEEE/RSJ*, Pittsburgh, Pennsylvania, August 1995.

[8] **Cooper**, D.W., **Wolfe**, H.L., **Yeh**, J.T., and **Miller**, R.J., "Surface Cleaning by Electrostatic Removal of Particles," *Aerosol Science and Technology*, vol. 13, 1990, pp. 116-123.

[9] **Masuda**, S., **Fujibayashi**, K., **Ishida**, K., and **Inaba**, H., "Confinement and Transportation of Charged Aerosol Clouds via Electric Curtain," *Electrical Engineering in Japan*, vol. 92, no. 1, 1972, pp. 43.

[10] **Gan-Mor**, and S., **Law**, S.E., "Frequency and Phase-Lag Effects on Transportation of Particulates by an AC Electric Field," *IEEE Transactions on Industrial Applications*, vol. 28, no. 2, March 1992, pp. 317-323.

[11] **Fuhr**, G., **Hagedorn**, R., and **Müller**, T., "Linear Motion of Dielectric Particles and Living Cells in Microfabricated Structures induced by Traveling Electric Fields," *Proc. IEEE Micro Electro Mechanical Systems Workshop*, Nara, Japan, January / February 1991, pp. 259-264.

[12] **Pethig**, R., "Applications of AC Electrical Fields to the Manipulation and Characterisation of Cells," *Conference Record 4th Toyota Conference*, October 1990.

[13] **Rao**, N.N., "Elements of Engineering Electromagnetics," *Prentice-Hall Inc. Fourth Edition*, 1994.